PRAMANA — journal of physics

Vol. 79, No. 3
September 2012
pp. 443–456

Electric field enhancement at multiple densities in laser-irradiated nanotube plasma

U CHAKRAVARTY*, P A NAIK and P D GUPTA
Laser Plasma Division, Raja Ramanna Centre for Advanced Technology, Indore 452 013, India
*Corresponding author. E-mail: uday@rrcat.gov.in

MS received 13 December 2011; accepted 10 May 2012

Abstract. The electric field enhancement inside a nanotube irradiated by intense ultrashort laser pulse ($\ll$1 ps) is calculated. The hollowness of the nanotubes determines the field enhancement and the electron density at which such structures exhibit resonance. The electric field in a nanotube plasma is shown to be resonantly enhanced at multiple densities during the two phases of interaction: the ionization phase and the hydrodynamic expansion phase. It is further shown that by a proper choice of hollowness of the nanotubes, a continued occurrence of the resonance over a longer time can be achieved. These properties make nanotubes efficient absorbers of intense ultrashort laser pulses.

Keywords. Nanotubes; absorption; field enhancement.

PACS Nos 36.40.Vz; 52.25.Mq; 52.38.Dx; 52.50.Jm

1. Introduction

Experimental investigations of interaction of intense ultrashort laser pulse with gas clusters and nanostructured targets are being widely pursued due to the enhanced energy coupling [1,2] leading to bright X-ray emission [3,4], generation of MeV ions [5], fusion neutrons [6], hot electrons [7] etc. To explain these features, a variety of models of the laser–cluster interaction have been put forward. These include: inner shell excitation [8], ionization ignition [9], collective electron dynamics [10], Coulomb explosion [11] and nanoplasma models [12]. The last one explains the maximization of the absorption cross-section and the electric field in the vicinity of Mie resonance at $3n_c$ in spherical clusters. Many experimental results concerning laser energy absorption and spectral characteristics [13–16] are observed to be consistent with this model. For cylindrical nanostructures, this maximization occurs when the electron density passes through $2n_c$ [17–19]. Elongated and pointed nanostructures (nanoprotrusions and nanorods) have shown enhanced X-ray and energetic particle emission and these have been attributed to the enhanced electric

field at the tip, also referred to as the 'lightning rod effect' [20–22]. It is desirable to design a nanotarget with a geometry which will enable even higher field enhancement when irradiated by ultrashort laser pulses for efficient X-ray and energetic particle generation. Unfortunately, the field enhancement in nanostructures discussed above is limited by their geometry and dielectric properties. Although the field is resonantly enhanced at Mie resonance in spherical clusters and nanorods at $3n_c$ and $2n_c$ respectively during the ionization and expansion phase, this resonance is at a density much lower than the solid density and also the resonance condition is short-lived ($\sim$ a few fs) [12,23]. Even more importantly, as the high density laser-heated cluster plasma expands, the electric field inside the cluster is shielded, i.e. the field inside the cluster is actually less than the applied laser field strength, and the field enhancement occurs only when the electron density is near to the resonance condition [12,18,19]. Further, a lower resonance electron density requires the laser-heated cluster to expand sufficiently long for the electron density to decrease and approach the resonance condition. This time required is typically $\sim$100 fs to 1 ps [13,24–27]. For ultrashort pulses of duration $<$100 fs, the clusters do not expand enough during the laser pulse to reach resonance at the peak of the pulse [13,27]. For maximum absorption and X-ray generation, it is therefore desirable that the resonance condition is met at the peak of the ultrashort laser pulse [13,24,25,27]. To meet this requirement, the laser pulse is generally stretched and there exists an optimum pulse duration for a given size of the cluster [13,23,24,27]. However, stretching of the pulse is not very desirable since it compromises the laser intensity as well as the duration of the resultant X-ray emission. In the light of the above facts, it would be ideal to have a structure that has resonance density close to the solid density, which will result in more absorption, electron generation and X-ray emission, as now more electrons would interact with the enhanced field. Moreover, a high resonance density means the resonance condition can be met even for pulses shorter than 100 fs, since now the nanostructure does not have to expand much to reach the resonance condition. It is further desirable that the chosen nanostructure has an extended resonance in time, so that the field enhancement continues during most of the entire hydrodynamic evolution.

Although a target with the above-mentioned features will be highly desirable, little work has been done for designing such nanostructure targets. Nevertheless, recently, some other kinds of nanostructures have been used for laser–matter interaction studies, especially ones which have hollow structures [28–35]. They show efficient high X-ray generation and hot electron generation, but their resonance densities have not been reported [28–35]. To name a few, the hollow nanotargets that have been used for experiments with intense short pulses are: fullerene [28], nanohole alumina [29], foam [30], nanobrush [31], carbon nanotubes (CNTs) [32,33] etc. The enhanced field and surface currents in hollow structures are believed to support hot electron generation and transport [31–35] necessary for fast ignition scheme in inertial confinement fusion, and also for efficient X-ray generation. The electric field enhancement in the nanostuctures makes the effective laser intensity on the target very high. Consequently, it leads to X-ray yield enhancement that is proportional to the rescaled enhanced intensity [36]. In the class of hollow targets, CNTs are very attractive for ultrashort laser–plasma interaction [32–34] as they can be easily produced in bulk quantities with controllable inner and outer diameters [37]. To understand the reason for the X-ray enhancement from nanotubes (as reported in refs [19,32,33]), it is necessary to investigate the effect of the hollow structure on the field

enhancement and to determine the optimum geometric parameters of the nanotubes for efficient absorption of ultrashort laser pulses ($\ll$1 ps).

In this paper, we calculate the electric field enhancement within a nanotube plasma, and find out the plasma density at which the field enhancement occurs. We find that nanotube has resonance density higher than a nanorod and it can even be tuned to be close to the solid density. Therefore, hollow structure helps in overcoming the limitation of a solid cluster or a nanorod whose resonance densities are much smaller than the solid density. Moreover, it is observed that instead of a single resonance density (e.g. $3n_c$ in spherical clusters [12] or $2n_c$ in a solid nanocylinder [17–19]), a nanotube shows field enhancement at two densities:

$$n_H = \frac{2n_c}{1-(a/b)} \qquad \text{and} \qquad n_L = \frac{2n_c}{1+(a/b)},$$

where a and b are the instantaneous inner and outer radii. The high-density resonance (n_H) occurs at a progressively higher density as one chooses nanotubes of increasing degree of hollowness (a/b). Multiple resonances can occur in hollow nanostructures during the ionization and hydrodynamic expansion phases. Another interesting feature arises from the fact that in an expanding heated nanotube, the plasma density as well as high resonance density (n_H) decrease with time. Simultaneous decrease in these two densities for nanotubes of certain degree of hollowness may allow continued occurrence of resonance for a much longer time.

2. Theoretical calculations

The interaction of ultrashort laser pulses with spherical clusters and nanorods is calculated by considering it as a nanoplasma [12–14,19,38]. The nanoplasma model follows a linear dielectric approach for nanoparticle interacting with intense pulse irradiation (typically $>10^{14}$ W/cm^2) [18,19,33,36]. For such a consideration, the general picture of a cluster interacting with the intense laser pulse is as follows. The laser-irradiated cluster ionizes instantaneously turning into a plasma ball at near solid density. The ion core, being massive, is stationary and the electron cloud oscillates (electrostatic oscillations) about the fixed ion core under the effect of laser field [39]. The cluster dipole moment and the internal electric field can be easily evaluated under the quasistatic approximation (the cluster size being much smaller than the incident laser wavelength) [12,36,39]. To obtain the cluster dipole moment, the displacement of the electron cloud with respect to the fixed ion core is found [39] and the internal electric field of clusters can also be derived. In another method, one solves the Laplace equation [12,18,19,36] taking the Drude dielectric function and Mie theory in dipole limit to obtain the resonance condition and the internal electric field distribution.

We now proceed on similar lines to calculate the electric field inside a laser-irradiated hydrodynamically evolving nanotube. Consider a nanotube with inner and outer radii a_0 and b_0 in an applied laser field of strength E_L ($E_L = (\hat{x}/2)(Ee^{i\omega t} + \text{c.c.})$). Let the laser field be oriented perpendicular to the axis of the nanotube. A field applied on a nanotube at any arbitrary direction has two components: one parallel to the axis and the other perpendicular to the axis. The component of the electric field applied parallel to the

nanotube axis is not enhanced [17–19]. The enhancement in the perpendicular component depends on the geometric and dielectric parameters of the nanotube.

Laser–nanotube interaction can be studied in two phases: the first is the ionization phase and the second is the hydrodynamic expansion phase. In the ionization phase, at the onset of the interaction of the nanotube with intense ultarshort laser pulse, there is plasma formation (the threshold of plasma formation is typically 10^{14} W/cm^2 for 100 fs pulse for planar solid and nanostructures [40]) which is crossed near the foot of the intense pulse. Therefore, the dielectric constant of the nanotubes instantaneously modifies and becomes metal-like or plasma-like because of the generation of free electrons [41,42]. The subsequent pulse further ionizes the nanostructure by optical field ionization and tunnel ionization, leading to the creation of a solid density plasma of density n_0 [12,13,19]. In the ionization phase, the geometry of the nanotubes is almost preserved during the interaction of the intense short pulse with the nanotubes since the temperature rise is not enough to cause sufficient hydrodynamic expansion for the structure to get modified in such short time-scales [12,18,19,26]. The expansion of the nanotubes is thus expected to be extremely slow during the ionization phase at the beginning of interaction and subsequently the temperature rises very quickly due to collisional absorption and maximum electron density is achieved near the peak of the pulse [12,26]. In the hydrodynamic expansion phase, the energy absorption and the consequent sharp rise of the plasma temperature causes the expansion of the nanoplasma, and the electron density of the cluster starts to decrease monotonically [12,26]. Since the plasma expansion takes place along the density gradient, the inner radius starts decreasing while the outer radius increases. Therefore, the expansion leads to the modification of the inner and outer radii to some instantaneous value a and b. It must be noted that during the ionization phase, the electron density increases monotonically (under the assumption that target geometry and inner and outer radii remain fixed). On the other hand, when the nanotube expands in the hydrodynamic expansion phase [23,38], the electron density decreases monotonically (under the assumption that no further ionization or recombination takes place) [13,19]. This modifies the dielectric constant ($\varepsilon = 1 - n_e/n_c$) of the nanotube plasma [13,19,20] during both the phases of interaction. Here n_e is the instantaneous electron density and n_c is the critical density for the laser.

Similar to a nanocluster or a nanorod, the electric field inside the hollow nanotube is calculated using the Laplace equation $\nabla^2 V = 0$ solved under the above-mentioned quasistatic approximation, where the outer radius considered is much smaller than the applied laser wavelength (i.e. $b \ll \lambda$). Solving this equation, one finds the dependence of the electric field in the nanotube on the instantaneous values of a, b, ε and E_L. Expanding in cylindrical coordinates and neglecting the Z variation (as the length of the cylinder is much larger compared to its outer diameter), the general solution is

$$V = K + \ln r + \sum_{n=1}^{\infty} \left(A_n r^n + B_n r^{-n}\right) \cos n\theta + \left(C_n r^n + D_n r^{-n}\right) \sin n\theta. \quad (1)$$

Applying appropriate boundary conditions, the potential can be shown to be

$$V_I = A_1 r \cos\theta, \qquad \text{for} \quad r \leq a \text{ (Region I)} \quad (2)$$

$$V_{\mathrm{II}} = \left(A_2 r + \frac{B_2}{r}\right)\cos\theta, \qquad \text{for} \quad a \le r \le b \text{ (Region II)} \tag{3}$$

$$V_{\mathrm{III}} = -E_{\mathrm{L}} r\cos\theta + \frac{B_3}{r}\cos\theta, \qquad \text{for} \quad r \ge b \text{ (Region III)}\,. \tag{4}$$

Using the continuity of D_n, E_t and potential V, one gets the four unknowns A_1, A_2, B_2, B_3 (all other A_i, B_i being zero) in terms of a, b and ε as

$$A_1 = \frac{-4E_{\mathrm{L}}\varepsilon}{(\varepsilon+1)^2 - (a/b)^2(\varepsilon-1)^2}, \tag{5a}$$

$$A_2 = \frac{-2E_{\mathrm{L}}(\varepsilon+1)}{(\varepsilon+1)^2 - (a/b)^2(\varepsilon-1)^2}, \tag{5b}$$

$$B_2 = \frac{-2E_{\mathrm{L}}a^2(\varepsilon-1)}{(\varepsilon+1)^2 - (a/b)^2(\varepsilon-1)^2}, \tag{5c}$$

$$B_3 = \frac{E_{\mathrm{L}}b^2\left(1-(a^2/b^2)\right)(\varepsilon^2-1)}{(\varepsilon+1)^2 - (a/b)^2(\varepsilon-1)^2}. \tag{5d}$$

The radial and azimuthal components of the electric field ($E_{\mathrm{r}} = -\partial V/\partial r$ and $E_\theta = -(1/r)(\partial V/\partial\theta)$) in the three regions can be derived from eqs (2), (3) and (4). The magnitudes of electric field ($\sqrt{E_{\mathrm{r}}^2 + E_\theta^2}$) in these three regions are thus given by

$$E_{\mathrm{I}} = A_1, \tag{6a}$$

$$E_{\mathrm{II}} = \sqrt{A_2^2 + \frac{B_2^2}{r^4} - \frac{2A_2B_2}{r^2}\cos 2\theta}, \tag{6b}$$

$$E_{\mathrm{III}} = \sqrt{E_{\mathrm{L}}^2 + \frac{B_3^2}{r^4} + \frac{2E_{\mathrm{L}}B_3}{r^2}\cos 2\theta}. \tag{6c}$$

We now calculate the electric field enhancement in laser-irradiated nanotube plasma. In Region I, the electric field is given by eq. (6a), and it is independent of r and θ. For Region II, one may define the root mean square (rms) electric field enhancement by taking the spatial average of the magnitude of field enhancement as

$$\langle E_{\mathrm{II}}/E_{\mathrm{L}}\rangle = \frac{1}{\pi\left(b^2-a^2\right)}\sqrt{\int_0^{2\pi}\int_a^b \left(\frac{E_{\mathrm{II}}}{E_{\mathrm{L}}}\right)^2 r\,\mathrm{d}r\,\mathrm{d}\theta}, \tag{7a}$$

$$= \frac{1}{E_L}\sqrt{A_2^2 + \frac{B_2^2}{a^2b^2}}. \tag{7b}$$

For a nanorod ($a = 0$), the above equations provide the electric field inside the nanorod to be $2E_L/(\varepsilon + 1)$, as expected [17,18]. By using the value of $\varepsilon = 1 - n_e/n_c$, where n_e is the electron density and n_c is the critical density, it is seen that the resonant field enhancement occurs at $2n_c$, in agreement with the earlier reported results [17–19].

Next, we may note from eqs (6a) and (7b), together with eqs (5a)–(5c), that the electric fields in Regions I and II will peak for certain values of (a/b) given by

$$\frac{a}{b} = \pm\left(\frac{\varepsilon + 1}{\varepsilon - 1}\right). \tag{8}$$

Therefore, the field enhancement in the case of nanotube plasma occurs at two densities:

$$n_H = \frac{2n_c}{1 - (a/b)}, \tag{9}$$

$$n_L = \frac{2n_c}{1 + (a/b)}. \tag{10}$$

It may be seen from eq. (9) that the higher resonance density (n_H) can be increased by choosing a nanotube of smaller wall thickness. This is in contrast with the case of solid clusters and nanorods, where the field enhancement occurs only in the vicinity of $3n_c$ and $2n_c$ respectively.

3. Results and discussion

From the preceding section, it is clear that the field enhancement depends on the ratio of the instantaneous inner and outer radii of the laser-irradiated nanotubes and the instantaneous dielectric constant of the plasma. First, one calculates the field enhancement factor during the ionization phase of laser–nanotube interaction where the electron density of the nanotube plasma monotonically increases as the laser pulse intensity increases. The nanotube gets ionized up to the solid density with no expansion (i.e. the initial inner and outer radii are a_0 and b_0) [13,19,43]. This is a valid assumption since the optical field ionization and tunnel ionization are instantaneous processes. Figure 1 shows the root mean square (rms) field enhancement during the ionization phase of laser-irradiated nanotubes of different degrees of hollowness (which is defined as the ratio of the initial inner and outer radii) subject to the condition that $b_0 \ll \lambda$, the assumption under which the Laplace equation was solved. For this calculation, one uses eq. (7b) and the value of ε is varied since n_e/n_c varies from 0 to 40 (n_0/n_c is taken as 40 for Ti:sapphire laser (800 nm) irradiation of CNTs). Four values of degree of hollowness (0, 0.5, 0.75 and 0.95) were chosen. It is seen from figure 1 that, for a nanorod, there is a single resonance at $2n_c$, and also the electric field is highly shielded as the electron density increases and approaches the solid density. It can also be seen that nanotubes show two resonances during ionization. To obtain a high electric field enhancement at a higher electron density, it is desirable to choose a nanotube with greater degree of hollowness. This brings out an important point

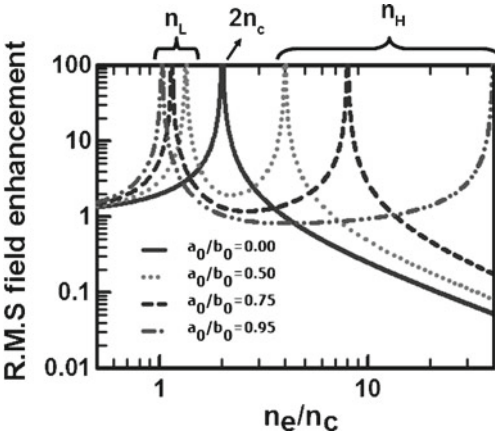

Figure 1. RMS field enhancement during the ionization phase of laser-irradiated nanotube plasma for fixed values of inner to outer radii nanotubes of different degrees of hollowness (a_0/b_0).

in the perspective of the spherical clusters and nanorods where the resonance condition ($3n_c$, $2n_c$) is met near the foot of laser pulse during the ionization phase. However, since the resonance is reached at low laser intensity (near the foot of the pulse), this resonance is of less significance [23,38]. It is desirable to meet the resonance condition at the peak of the laser pulse. If the resonance density is enhanced by choosing a hollow nanostructure, the resonance condition can be met when the applied field is also high [13,24,25,27]. Therefore, even in the ionization phase, one can make the resonance happen near the peak of the pulse so that it will have a significant role in the interaction with the nanotube.

Next, for the other phase of laser–nanotube interaction where one considers the hydrodynamic evolution, one can consider a zero time to mark the onset of expansion and variation of inner and outer radii of the nanotube with time. One can define the zero time as the time when the nanotube plasma is ionized up to the solid density n_0 assuming no expansion has occurred (i.e. the initial inner and outer radii are at a_0 and b_0) [13,19,43]. For calculating the initial value of ε, n_0/n_c is taken as 40. This will help in identifying the class of nanotubes with same degree of hollowness (a_0/b_0) for maximum initial field enhancement. Figure 2 shows variation of the initial field enhancement factor with the degree of hollowness (a_0/b_0) in Regions I and II. The value of a_0/b_0 lies between 0 and 1, for a nanorod having the degree of hollowness $a_0/b_0 = 0$. It is clearly seen that for a nanorod the field is highly shielded. It is also seen that the field in Region I is higher than that in Region II. Further, for smaller values of a_0/b_0, there is a shielding of the applied electric field. However, as the degree of hollowness increases, field enhancement occurs. The maximum enhancement occurs for

$$\frac{a_0}{b_0} = \frac{n_0 - 2n_c}{n_0}. \tag{11}$$

As can be seen from eq. (9), this condition corresponds to the occurrence of the high-density resonance at the solid density n_0. Beyond this value of a_0/b_0, the field enhancement starts reducing.

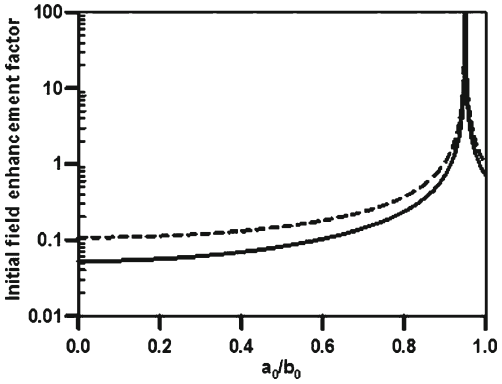

Figure 2. Initial field enhancement factor as a function of a_0/b_0 in two regions of the nanotube: (Region I) dotted curve ($r < a_0$), (Region II) solid curve ($a_0 < r < b_0$). Maximum initial field enhancement occurs for $(a_0/b_0) = (n_0 - 2n_c)/n_0$.

Now we examine the temporal evolution of the rms electric field during the expansion phase in the nanotube plasma and also estimate the time-scales of resonance, as was done for clusters or nanofibres [19,24,43]. This is done by assuming constant temperature. As the plasma expands along the density gradient (perpendicular to the nanotube axis), the instantaneous inner radius a decreases and is $= a_0 - c_s t$ and outer radius b increases and is $= b_0 + c_s t$, where $c_s = \sqrt{ZkT_e/M_i}$ is the plasma expansion speed and where M_i is the ion mass. The value of c_s can be estimated from the work of Issac *et al* [44] who have done experiments on gas cluster using Ti:Sapphire laser with the duration ranging from 60 fs to 2 ps, and intensity up to 10^{18} W/cm^2. They have predicted a nearly constant electron temperature (between 1 and 2 keV) from experiments and simulations for the range of pulse duration in their experiments. Taking the typical value of plasma temperature of $\sim$1 keV from their work, we estimate c_s to be $\sim$100 nm/ps [19]. Of course, c_s will have some variation during the hydrodynamic expansion, but a constant value of c_s for a given average electron temperature helps in predicting the time-scale at which the resonance would occur. For example, various experiments on spherical clusters and nanofibres have shown that an assumption of constant c_s helps in predicting the resonance time-scales quite accurately [13,19]. Moreover, the simulations done by Ditmire *et al* [45] and Liu *et al* [26] show that the ion velocity c_s is extremely low initially during the ionization phase and after that it increases very rapidly when the electron density becomes close to solid density (this happens approximately near the peak of the laser pulse), and after this c_s is almost constant. The electron density gradually decreases as the cluster expands with a variation discussed shortly. On the basis of this picture, it is a good approximation to consider the zero time as that time when the nanotube plasma is at solid density n_0 with a given inner and outer radii a_0 and b_0 and then it starts expanding eventually leading to the monotonic decrease of the electron density [18,19,26,43].

An important point during the hydrodynamic expansion of the nanotube plasma is the 'void closure', i.e. when $a = 0$. The time required for void closure (t_v) is a_0/c_s. If the void closure occurs before the condition for high-density resonance is reached, one may term the nanotube as a 'thick' nanotube. On the other hand, if the void closure takes

place after the occurrence of high-density resonance, the nanotube may be referred to as a 'thin' nanotube. We first consider a thick nanotube. Before the void closure, the plasma density varies with time as $n_e = n_0(b_0 - a_0)/(b_0 - a_0 + 2c_s t)$, and after the void closure, it varies as $n_e = n_0(b_0^2 - a_0^2)/(a_0 + b_0 + c_s\tau)^2$, where τ in the last expression is the time after void closure). Once the void closure occurs, the nanotube plasma behaves like a nanorod which will show resonance at $2n_c$. Next, in the case of a thin nanotube, the time taken by the nanotube plasma to reach the high density (n_H) resonance is

$$t_H = \frac{1}{c_s}\left[(b_0 - a_0)\,\frac{n_0}{2n_c} - b_0\right].$$

By comparing this time with the time of void closure, it is easily seen that the high-density resonance will occur before void closure if $(a_0/b_0) > (n_0 - 2n_c)/(n_0 + 2n_c)$. Further, in a real situation, $t_H > 0$. This implies that $(a_0/b_0) < (n_0 - 2n_c)/n_0$. It can be shown that if this condition is satisfied, then the low-density (n_L) resonance also occurs before the void closure. Therefore, two resonances occur only when

$$\frac{n_0 - 2n_c}{n_0 + 2n_c} < \frac{a_0}{b_0} < \frac{n_0 - 2n_c}{n_0}.$$

In the thin nanotube category, we may identify two particular situations, viz. $(a_0/b_0) = (n_0 - 2n_c)/n_0$ as in eq. (11), and the other being $(a_0/b_0) > (n_0 - 2n_c)/n_0$. As seen from figure 2 and discussed earlier, the first condition $(a_0/b_0) = (n_0 - 2n_c)/n_0$ corresponds to the occurrence of high-density resonance at the solid density. Such a nanotube may be referred to as 'resonant' nanotube. Finally, when $(a_0/b_0) > (n_0 - 2n_c)/n_0$, the high-density resonance does not occur at all, and only the low-density resonance condition is fulfilled. We may refer to such a nanotube as 'ultrathin'. Thus, the nanotubes can be categorized as:

Thick nanotube:

$$0 < \frac{a_0}{b_0} < \frac{n_0 - 2n_c}{n_0 + 2n_c}. \tag{12}$$

Thin nanotube:

$$\frac{n_0 - 2n_c}{n_0 + 2n_c} < \frac{a_0}{b_0} < \frac{n_0 - 2n_c}{n_0}. \tag{13}$$

Ultrathin nanotube:

$$\frac{a_0}{b_0} > \frac{n_0 - 2n_c}{n_0}. \tag{14}$$

Resonant nanotube:

$$\frac{a_0}{b_0} = \frac{n_0 - 2n_c}{n_0}. \tag{15}$$

Using eqs (5b), (5c) and (7b), one can plot the rms electric field enhancement evolution for nanotubes with initial inner and outer radii a_0 and b_0 respectively, while they expand

after being irradiated by an intense ultrashort laser pulse. The initial maximum plasma electron density is chosen as $n_0/n_c = 40$ and the expansion speed $c_s = 100$ nm/ps [44]. We also take into account the fact that hydrodynamic evolution causes the instantaneous inner radius a to decrease as $a_0 - c_s t$ and outer radius b to increase as $b_0 + c_s t$ and this causes the decrease of electron density and the dielectric constant (ε) modifies accordingly. Figure 3 shows the calculated variation of the rms electric field enhancement in Region II for thick and thin carbon nanotubes. Figure 3a depicts the case of a thick nanotube ($a_0 = 40$ nm, $b_0 = 50$ nm), showing the occurrence of void closure at 400 fs, followed by $2n_c$ resonance at 840 fs. Figure 3b shows the electric field evolution for a thin nanotube ($a_0 = 47$ nm, $b_0 = 50$ nm). It is noted that while for the thick nanotube there was an initial field shielding and the field enhancement occurred only near $2n_c$, the field inside the thin nanotube is highly enhanced from the very beginning of heating and expansion and the enhancement takes place throughout the expansion of the nanotube. The high (H) and low (L) density resonances are observed at 100 fs and 335 fs respectively, prior to the void closure (V) at 470 fs. Figure 3c shows the electric field evolution for ultrathin nanotube ($a_0 = 48$ nm, $b_0 = 50$ nm). It shows the occurrence of the low-density resonance (L) at 250 fs, while the void closure (V) occurs at 480 fs. Like the

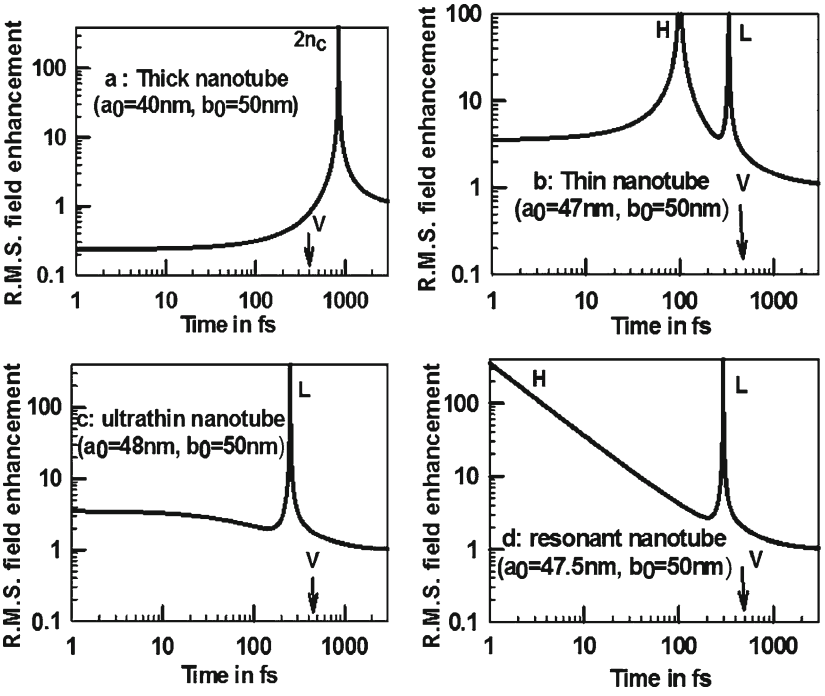

Figure 3. Time evolution of the electric field in nanotubes of different sizes: (**a**) Thin nanotube, (**b**) thick nanotube, (**c**) ultrathin nanotube and (**d**) resonant nanotube (all for $n_0/n_c = 40$, $c_s = 100$ nm/ps). The points H, L and V indicate the time corresponding to the occurrence of higher-density resonance, lower-density resonance and void closure respectively.

thin nanotube, even in ultrathin nanotube the field enhancement exists at all instants of the expansion. Finally, figure 3d shows the electric field evolution of a resonant nanotube ($a_0 = 47.5$ nm, $b_0 = 50$). It is seen that the high-density resonance (H) occurs over an extended time period from the beginning. The low-density resonance (L) occurs at 295 fs and void closure at 475 fs. Thus, in all the cases of thin nanotube, there is a greater field enhancement compared to the thick nanotube.

An important aspect of the nanotube–laser interaction is the fact that as the nanotube (with appropriate choice of a_0 and b_0) expands, the higher density resonance will progressively occur at lower densities, so that the resonance condition can be sustained over a longer time. This is clearly seen in figure 4 which depicts the time evolution of the resonance densities of different nanotubes (thick, thin, ultrathin and resonant), plotted along with their density evolution for $n_0/n_c = 40$ and $c_s = 100$ nm/ps. The point of intersection of the decreasing nanotube density with evolving resonance density gives the time of occurrence of resonance. Figure 4a shows that the void closure (V) in the case of thick nanotube ($a_0 = 40$ nm, $b_0 = 50$ nm) takes place before the occurrence of the resonance condition and the resonant density becomes $2n_c$, like in a solid nanorod. In addition, the time duration over which the nanotube plasma density is close to the resonance density is small. Figure 4b for thin nanotube ($a_0 = 47$ nm, $b_0 = 50$ nm) shows the occurrence of both higher and lower density resonances (H,L) before the void closure (V) occurs. In

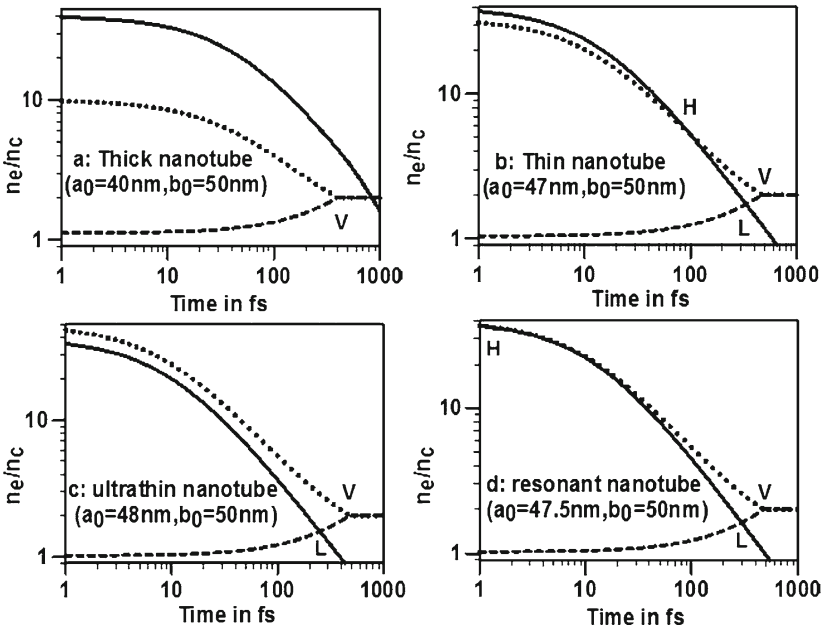

Figure 4. Time evolution of the nanotube density (solid curve) along with that of the higher resonance density (dotted curve) and the lower resonance density (dashed curve) for (**a**) thick, (**b**) thin, (**c**) ultrathin and (**d**) resonant nanotubes. The points H, L and V indicate the time corresponding to the occurrence of higher density resonance, lower density resonance and void closure respectively.

this case, the plasma density remains in the vicinity of the high resonance density for a longer time. Figure 4c shows that in the case of ultrathin nanotube ($a_0 = 48$ nm, $b_0 = 50$ nm), only the low-density resonance (L) takes place before void closure (V) and the resonance condition is met over a small time. Figure 4d shows that in the case of 'resonant' nanotube ($a_0 = 47.5$ nm, $b_0 = 50$ nm), the high-density resonance starts from the very onset of expansion, and the resonance continues for a very long time compared to the other categories of nanotubes. These figures (figures 4a–c) also show the number of resonances shown by thick, thin and ultrathin tubes, as were seen earlier in figures 3a–c. The overall analysis shows that the fact that the hollow structure has various advantages over clusters or nanorods as resonance density of a nanotube can be tuned close to the solid density and the resonance condition can be met for pulses shorter than 100 fs. In addition to this, there are resonances during the ionization and expansion phases, along with continued occurrence of high-density resonance for a nanotube with a particular degree of hollowness. Finally, since the electric field inside a structure governs the absorption, electron, ion and X-ray generation, large field enhancement in laser-irradiated nanotubes make them very interesting targets from the application point of view.

4. Conclusion

In conclusion, we have studied the electric field enhancement inside the nanotube plasma irradiated by intense short pulse laser. The hollowness of the nanotubes determines the field enhancement and the electron density at which such structures exhibit resonance. It is found that a nanotube exhibits two resonances at two electron densities during the ionization phase. During the hydrodynamic expansion phase also, a thin nanotube exhibits resonant field enhancement at two densities (depending on its inner and outer radii). There exists a particular ratio of the inner to outer radii of the nanotube where the field enhancement starts right at the solid density which may continue for a much longer time as the higher resonance density and the nanotube density decrease simultaneously during the expansion of the heated nanotube. While detailed theoretical calculations and computer simulations may be necessary to obtain exact quantitative information, the physical effects are quite well illustrated by taking simple analytical treatment and typical parameters of laser–nanotube interaction. The observed features make nanotubes of appropriately chosen inner and outer radii an attractive target for efficient absorption of intense ultrashort laser pulses. It will also be interesting to study the interaction of nanotubes with an intense few-cycle laser pulse since the hydrodynamic motion is almost frozen in those time-scales and the pulse interacts with a solid density plasma. In general, these calculations can also be extended to design efficient carbon nanotubes-based field emitters.

Acknowledgements

The authors acknowledge useful discussions with Ajeet Kumar, Usha Chakravarty and Shreekant Barnwal of RRCAT, India.

References

[1] T Ditmire, R A Smith, J W G Tisch and M H R Hutchinson, *Phys. Rev. Lett.* **78**, 3121 (1997)
B Ziaja, H Wabnitz, F Wang, E Weckert and T Möller, *Phys. Rev. Lett.* **102**, 205002 (2009)

[2] T Palchan, S Peckerand, Z Henis, S Eisenmann and A Zigler, *Appl. Phys. Lett.* **90**, 041501 (2007)
G Kulcsar, D AlMawlawi, F W Bundnik, P R Herman, M Moskovits, L Zhao and R S Marjoribanks, *Phys. Rev. Lett.* **84**, 5149 (2000)

[3] M M Murnane, H C Kapteyn, S P Gordon, J Bokor and E N Glytsis, *Appl. Phys. Lett.* **62**, 1068 (1993)

[4] F Dorchies, F Blasco, C Bonté, T Caillaud, C Fourment and O Peyrusse, *Phys. Rev. Lett.* **100**, 205002 (2008)

[5] A Zigler, T Palchan, N Bruner, E Schleifer, S Eisenmann, M Botton, Z Henis, S A Pikuz, A Y Faenov Jr, D Gordon and P Sprangle, *Phys. Rev. Lett.* **106**, 134801 (2011)

[6] T Ditmire, J Zweiback, V P Yanovsky, T E Cowan, G Hays and K B Wharton, *Nature* **398**, 489 (1999)

[7] Y L Shao, T Ditmire, J W G Tisch, E Springate, J P Marangos and M H R Hutchinson, *Phys. Rev. Lett.* **77**, 319007 (1996)

[8] A McPherson, B D Thompson, A B Borisov, K Boyer and C K Rhodes, *Nature* **370**, 631 (1994)

[9] E M Snyder, S A Buzza and A W Castleman, *Phys. Rev. Lett.* **77**, 3347 (1996)

[10] U Saalmann and J M Rost, *Phys. Rev. Lett.* **91**, 223401 (2003)

[11] T Ditmire, J W G Tisch, E Springate, M B Mason, N Hay, R A Smith, J Marangos and M H R Hutchinson, *Nature* **386**, 54 (1997)

[12] T Ditmire, T Donnelly, A M Rubenchik, R W Falcone and M D Perry, *Phys. Rev.* **A53**, 3379 (1996)

[13] J Zweiback, T Ditmire and M D Perry, *Phys. Rev.* **A59**, R3166 (1999)

[14] H Singhal, V Arora, P A Naik and P D Gupta, *Phys. Rev.* **A72**, 43201 (2005)

[15] S Sailaja, R A Khan, P A Naik and P D Gupta, *IEEE Trans. Plasma Sci.* **33**, 1006 (2005)

[16] A M Bystrov and V B Gildenburg, *Phys. Rev. Lett.* **103**, 083401 (2009)

[17] G D Mahan, *Phys. Rev.* **B74**, 033407 (2006)

[18] U Chakravarty, V Arora, J A Chakera, P A Naik, H Srivastava, P Tiwari, A Srivastava and P D Gupta, *J. Appl. Phys.* **109**, 053301 (2011)

[19] U Chakravarty, P A Naik, B S Rao, V Arora, H Singhal, G M Bhalerao, A K Sinha, P Tiwari and P D Gupta, *Appl. Phys. B: Lasers and Optics* **103**, 571 (2011)

[20] P P Rajeev, P Taneja, P Ayyub, A S Sandhu and G R Kumar, *Phys. Rev. Lett.* **90**, 115002 (2003)

[21] S Kim, J Jin, Y J Kim, I Y Park, Y Kim and S W Kim, *Nature* **453**, 757 (2008)

[22] S Bagchi, P P Kiran, M K Bhuyan, S Bose, P Ayyub, M Krishnamurthy and G R Kumar, *Appl. Phys. Lett.* **90**, 141502 (2007)

[23] H M Milchberg, S J McNaught and E Parra, *Phys. Rev.* **E64**, 056402 (2001)

[24] J Jha and M Krishnamurthy, *Appl. Phys. Lett.* **92**, 191108 (2008)

[25] E Parra, I Alexeev, J Fan, K Y Kim, S J McNaught and H M Milchberg, *J. Opt. Soc. Am.* **B20**, 118 (2003)

[26] J Liu, R Li, P Zhu, Z Xu and J Liu, *Phys. Rev.* **A64**, 033426 (2001)

[27] F Dorchies, T Caillaud, F Blasco, C Bonté, H Jouin, S Micheau, B Pons and J Stevefelt, *Phys. Rev.* **E71**, 066410 (2005)

[28] R A Ganeev, L B Elouga Bom, J Abdul-Hadi, M C H Wong, J P Brichta, V R Bhardwaj and T Ozaki, *Phys. Rev. Lett.* **102**, 013903 (2009)

[29] T Nishikawa, H Nakano, K Oguri, N Uesugi, K Nishio and H Masuda, *J. Appl. Phys.* **96**, 7537 (2004)
[30] T Nishikawa, H Nakano, H Ahn and N Uesugi, *Appl. Phys. Lett.* **70**, 1653 (1997)
[31] Z Zhao, Lihua Cao, Leifeng Cao, J Wang, W Huang, W Jiang, Y He, Y Wu, B Zhu, K Dong, Y Ding, B Zhang, Y Gu, M Y Yu and X T He, *Phys. Plasmas* **17**, 123108 (2011)
[32] T Nishikawa, S Suzuki, Y Watanabe, O Zhou and H Nakano, *Appl. Phys.* **B78**, 885 (2004)
[33] S Bagchi, P P Kiran, M K Bhuyan, M Krishnamurthy, K Yang, A M Rao and G R Kumar, *Phys. Plasmas* **18**, 014502 (2011)
[34] Y Ji, G Jiang, W Wu, C Wang, Y Gu and Y Tang, *Appl. Phys. Lett.* **96**, 041504 (2010)
[35] Lihua Cao, Y Gu, Z Zhao, Leifeng Cao, W Huang, W Zhou, H B Cai, X T He, Wei Yu and M Y Yu, *Phys. Plasmas* **17**, 103106 (2010)
[36] P P Rajeev, P Ayyub, S Bagchi and G R Kumar, *Opt. Lett.* **29**, 22 (2004)
[37] L Kim, Eun-mi Lee, S-J Cho and J S Suh, *Carbon* **43**, 1453 (2005)
[38] K Y Kim, I Alexeev, V Kumarappan, E Parra, T Antonsen, T Taguchi, A Gupta and H M Milchberg, *Phys. Plasmas* **11**, 2882 (2004)
[39] M Kumar and V K Tripathi, *Phys. Plasmas* **16**, 123111 (2009)
[40] P P Rajeev, S Sengupta, A Das, P Taneja, P Ayyub, P K Kaw and G R Kumar, *Appl. Phys.* **B80**, 1015 (2005)
[41] M Huang, F L Zhao, Y Cheng, N Xu and Z Xu, *Phys. Rev*. **B79**, 125436 (2009)
[42] M Huang, F L Zhao, Y Cheng, N Xu and Z Xu, *ACS Nano.* **3**, 4062 (2009)
[43] Y Liu, Q Dong, X Peng, Z Jin and J Zhang, *Phys. Plasmas* **16**, 043301 (2009)
[44] R C Issac, G Vieux, B Ersfeld, E Brunetti, S P Jamison, J Gallacher, D Clark and D A Jaroszynski, *Phys. Plasmas* **11**, 3491 (2004)
[45] T Ditmire, J W G Tisch, E Springate, M B Mason, N Hay, J P Marangos and M H R Hutchinson, *Phys. Rev. Lett.* **78**, 2732 (1997)